**Earthquakes and Structures**, *Vol. ????, No. ???? (????) 1–21*
DOI: http://dx.doi.org/???? 

# Parametric seismic evaluation of highway overpass bridges in moderate seismic areas

József Simon*[1] and László Gergely Vigh[1a]

[1]*Department of Structural Engineering, Budapest University of Technology and Economics, Budapest, Műegyetem rkp. 3-5.,H-1111, Hungary*

*(Received ????, Revised ????, Accepted ????)*

**Abstract.** Prior to modern seismic provisions, several bridges were not designed for seismic actions in moderate seismic areas. Precast multi-girder and slab bridges are typical highway overpass structures, they have a significant contribution to national bridge stocks. Since the seismic behavior is questionable, a preliminary parametric study is conducted to determine critical configurations and components. The results indicate that the behavior of the abutments, backfill soil, superstructure and foundation is normally satisfactory; however, the superstructure-abutment joints are critical for both single and multi-span bridges, while the piers are also critical for longer multi-span configurations. The parametric results provide a solid basis both for detailed seismic assessment and development of design concepts of newly built structures in moderate seismic zones.

**Keywords:** Seismic analysis; parametric analysis; multi modal response spectrum analysis; seismic performance; bridge engineering; moderate seismicity

## 1. Introduction

In modern seismic codes (e.g. CEN (2008a, b), BSSC (2009)) seismic design of bridges is prescribed in moderate seismic regions; however a large portion of existing structures were non-seismically designed in these areas due to the lack of proper seismic provisions prior to the introduction of modern standards. Several studies (Choi and Jeon 2003, Nielson 2005, Ramanatan *et al.* 2012, Zsarnóczay *et al.* 2014, Simon *et al.* 2015) have shown that existing road bridges may be vulnerable even in moderate seismic regions. This high vulnerability stems not only from the lack of seismic design and detailing, but also from the fact that the seismic hazard has been recently revised in many countries of moderate seismicity (e.g. Austria, Belgium, Czech Republic, Germany, Slovakia, Slovenia, Switzerland). New seismic hazard maps were created showing an increased hazard (Solomos *et al.* 2008), therefore additional seismic demands are imposed on the structures compared to the previous standards. This latter issue is a subject of a huge debate among civil engineers and authorities;

*Corresponding author, Ph.D., E-mail: simon.jozsef@epito.bme.hu
[a]Ph.D., E-mail: vigh.l.gergely@epito.bme.hu


http://www.techno-press.org/?journal=sem&subpage=8 ISSN: 1225-4568(Print), 1598-6217(Online)

the structural safety of existing structures against severe earthquake-induced damage and ultimately collapse is questionable (Borzi *et al.* 2013). Therefore, in these regions, where seismic design is practically non-existent, there is a need for a fast and overall, nationwide seismic performance evaluation of the most important bridge types to provide: 1) insight on the seismic risk for the authorities; 2) information on the seismic behavior and the critical bridge configurations and components for practicing engineers, which can be useful in case of a new bridge design.

The most common structural types on highways are the precast multi-girder (PMG) and reinforced concrete slab bridges; these typologies are widely employed in several moderate seismic regions around the world (Connal 2014, Nielson 2005, Pinto and Franchin 2010). For instance, evaluation of a representative bridge database in Hungary (HTA 2016) shows that besides bridges with conventional bearings, the number of PMG and slab bridges with monolithic joints has a contribution of more than 70% to the national bridge stock.

There are a few examples of comprehensive seismic performance evaluation of highway bridges (e.g. in the US (Nielson 2005), Italy (Borzi *et al.* 2015), Greece (Moschonas *et al.* 2009), Turkey (Avşar *et al.* 2015)), however there are several reasons why the results of these studies cannot be adapted: 1) the higher seismicity of the mentioned countries in Europe results in different design traditions, therefore structural characteristics and details; 2) PMG and slab bridges examined in this study are dominantly continuous and built with monolithic joints, while simply supported versions are more preferred in the mentioned regions; 3) the studies do not cover all the possible bridge configurations; 4) the vulnerability depends on the applied seismic actions, which should be determined considering the seismic characteristics and site properties, thus results are expected to differ in moderate seismic zones.

The objective of this study is to investigate the seismic performance of typical PMG and slab bridges. A parametric seismic analysis and standard evaluation per the EC8 standard are carried out. This approach is usually adopted for preliminary seismic evaluation of structures (Fagà *et al.* 2016). Main variable parameters (number of spans, span of single bay, deck width, pier height) are selected to represent a wide range of different configurations that may be found on highways in moderate seismic regions. Based on the results, critical layouts and components are determined, demand-capacity ratios of bridge components are calculated. A possible application of the parametric results is also illustrated with an example: a nationwide seismic performance evaluation is performed for Hungarian road bridges; a first estimation is given for the number of critical bridges considering the whole bridge stock.

## 2. Description of the examined bridge configurations

Both PMG and slab bridges are constructed with monolithic joints of which there are two typical types: 1) piers are joined directly to the reinforced concrete deck (Fig. 1a) in case of slab bridges; 2) vertical reinforcement is applied at the pier cap (Fig. 1b) of PMG bridges and at the abutments (Fig. 1c) of PMG and slab bridges to transfer lateral forces only. *Type 1* joints can be characterized with complex behavior transferring both shear forces and bending moments from the superstructure to the piers, while the behavior of *Type 2* joints is simpler. Since only shear reinforcement is applied, they can be characterized with semi-

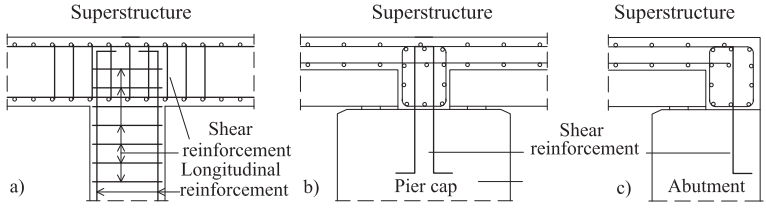


Fig. 1 Monolithic joint types. a) Piers are joined directly to the deck (*Type 1*; slab bridges). Shear reinforcement is applied between: b) the deck and the pier cap (*Type 2*; PMG bridges); c) the deck and the abutment (*Type 2*; both PMG and slab bridges).

rigid flexural behavior. The flexural stiffness is negligible compared to that of the adjacent structural elements, thus it is best approximated as hinged (Fennema *et al.* 2005).

Fig. 2a shows the general layout of PMG bridges. They are constructed as follows. In the first construction steps, the substructure is created (piles, pile cap, abutments and piers, and finally the pier cap beam); vertical reinforcements are extended from the abutment and pier cap. Precast beams are placed on the pier cap beam and on the abutments. The last step is to position the reinforcements of the deck, then the monolithic joints and the concrete deck are constructed with cast-in-situ concrete. Typical shear reinforcements of the monolithic *Type 2* joints are $\phi$16/150 at the abutment and 2$\phi$16/150 at the piers. Since there are various girder types (I,T,U etc.), a statistical analysis is carried out based on the Hungarian bridge database (HTA 2016) to determine the average stiffness properties of different girder bridges as the function of the span length. These properties are used to construct an equivalent slab for the numerical calculations (see Fig. 2b). Additional permanent load of the superstructure is 750 kg/m railing and 400 kg/m$^2$ pavement. Piers are constructed as multi-column bents with 3-4 m transverse distance. Longitudinal reinforcement ratio is typically 1%, while minimal shear reinforcement (mostly $\phi$12/150) is applied due to the low shear forces in conventional design situations (e.g. traffic loads).

Since these bridges are highly popular on highways, cross section of the piers (0.6 m x 0.9 m) and the pier cap (1.0 m x 1.2 m) and the dimensions of the abutments (1.0 m x 2.0 m) are more or less the same for all structures for the efficient reusability of formwork. Accordingly, pier and cap beam cross-section, abutment geometry are considered fixed during the studies. The foundation system is mostly pile foundation, the assumed layouts for different deck widths are shown in Fig. 2c. The input parameters of the parametric study are presented in Table 1 where the notations for different configurations are also indicated (e.g. a 14 m wide, 3-span bridge with 6 m pier height and 20 m span length is referred to as W14S3P06L20).

Table 1 Input parameters for the parametric study and notations for different configurations.

| | Width [m] | Number of spans[-] | Pier height [m] | Span length [m] |
|---|---|---|---|---|
| Values | 8, 14, 20 | 2, 3, 4 | 2, 5, 8 | 15, 30 |
| Notations | W08, W14, W20 | S2, S3, S4 | P02, P05, P08 | L15, L30 |

Slab bridges are cast-in-situ monolithic reinforced concrete structures commonly constructed as highway overpass bridges along with PMG bridges. Their construction requires stand- and formwork, thus the construction time is longer than in case of PMG bridges. The

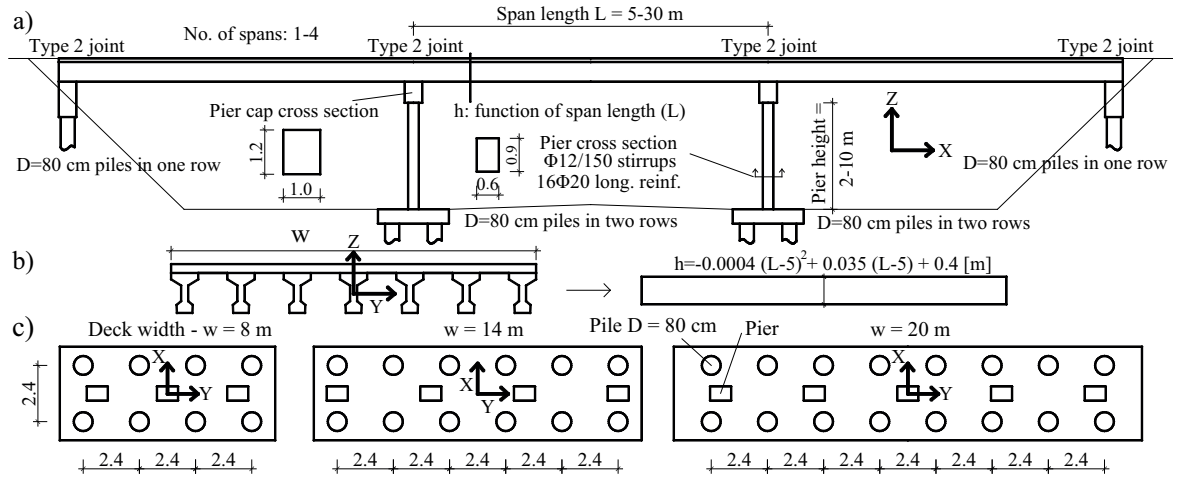


Fig. 2 General layout of PMG bridges: a) side-view of the bridge; b) typical cross section; c) applied pile foundation arrangements for different bridge widths.

general layout is shown in Fig. 3a. The global geometry is usually the same as of PMG bridges, thus the examined configurations and the parametric space are assumed to be the same in this study (see Table 1). Nonetheless, fundamental differences affecting the behavior of slab bridges should be highlighted. Note that there is no pier cap, piers are connected directly to the deck with a monolithic joint which can transfer not only shear forces but also bending moments (monolithic joint *Type 1*). However, the joints at the abutments are constructed with one layer of vertical bars only, characterized by a similar behavior as PMG bridge joints (monolithic joint *Type 2*). The stiffness and mass of the deck is calculated considering typical slab bridge cross-sections for different deck widths (Fig. 3b). The structural height is determined as the function of span length.

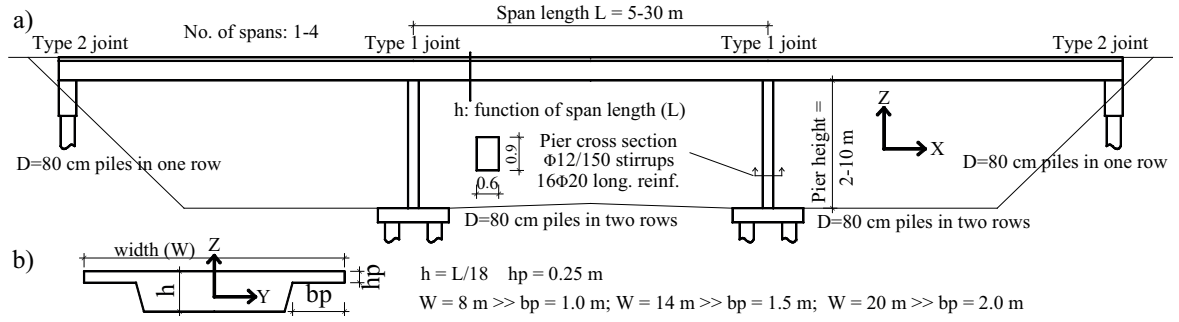


Fig. 3 General layout of SLAB bridges: a) side-view of the bridge; b) general cross-section.

## 3. Applied procedure for parametric seismic analysis

State of the art seismic vulnerability evaluation techniques are based on analytical fragility curves (Billah and Alam 2015). Damage evaluation is necessary for estimating loss and eco-

nomic consequences, however, to estimate the occurrence probability of different damage levels, each bridge has to be modeled with high fidelity and reliable input values (Simon and Vigh 2016). In typical moderate seismic regions, seismic design is practically non-existent. Therefore, prior to detailed analyses, it is advantageous to perform a preliminary study to highlight critical configurations, and most importantly to give an estimation of possibly critical structures, enabling the authorities to make decisions about further actions.

Several simplified vulnerability assessment methodologies have been worked out based on bridge inspection without complex calculations (Kibboua *et al.* 2014). These methodologies (Kawashima and Unjoh 1990, Gilbert 1993, OFROU 2005, Marchand *et al.* 2006) apply a scoring system and vulnerability parameter, which are determined considering the main aspects of bridge vulnerability: intensity of earthquake, soil conditions, main structural attributes etc. The disadvantage of this approach is two-fold: 1) it requires comprehensive inspection of each bridge (which can be a time-consuming procedure); 2) it is based on regression analysis on bridge damage data, thus the reliability of the evaluation is questionable, especially if bridges with significantly different main structural attributes are investigated.

A transitional approach between detailed fragility analysis and simplified inspection-based evaluation is the application of a simplified yet informative analysis procedure. The main structural attributes (e.g. pier height or span length) of PMG and slab bridges are diverse, thus a parametric evaluation is necessary to determine which configurations may be vulnerable and require further detailed analysis. Accounting for these requirements, an intensity based approach is adopted in this study, as it was already shown to be efficient for parametric analyses of a large dataset of structures (Fagà *et al.* 2016). A typical moderate PGA value of 1.5 $m/s^2$ related to the EC8-1 non-collapse criteria is considered (PGA hazard is computed at 10% exceedance rate in 50 years). Time-efficient multi modal response spectrum analysis (MMRSA) is used to compute seismic demands (Chopra 1995). Although MMRSA cannot capture non-linear behavior, the short computational time ensures to cover a wide parametric field, and provides insight about the governing seismic demands.

An OpenSees procedure is written by the authors (Simon and Vigh 2014) to carry out MMRSA per EC8-1. The procedure calculates the necessary number of modes (i.e. the 90% modal mass rule is applied), then spectrum analysis is carried out. Modes are combined with the Complete Quadratic Combination method, while the combination of results of each direction is based on the Square Root of the Sum of the Squares approach. The applied acceleration response spectrum (Fig. 4) assumes a reference soil type C and Type 2 spectral shape per EC8-1, well reflecting typical circumstances. The bridges are considered as ordinary bridges of normal importance, thus an importance factor of 1.0 is used to determine the seismic load. A behavior factor q=1.0 is applied as it is suggested by EC8-2 for bridges with a deck connected to both abutments with monolithic joints.

## 4. Numerical model

A three dimensional beam-element model is created in OpenSees (McKenna *et al.* 2010). Considering the linear nature of the analysis method, the structural elements (superstructure, piers and abutments; Fig. 5) are modeled with a simple 1-D Euler-Bernoulli beam element,

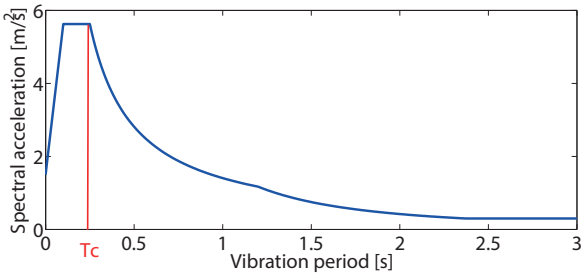


Fig. 4 Applied standard Type 2 acceleration response spectrum (PGA = 1.5 m/s$^2$, soil type C, q=1).

since the flexure-shear interaction (Kagermanov and Ceresa (2016); Ceresa *et al.* (2009)) is not accounted for due to the expected elastic behavior. The beam elements are placed in the center of mass, eccentricity between the member axes is bridged over with rigid elements. A typical mesh size of 0.25 m results in approximately 100 to 1000 nodes (600-6000 DOFs), which is found sufficient to efficiently achieve results with an acceptable accuracy. The mass of the structure and the additional dead load (pavement, rails etc.) are lumped at nodes.

Although, non-linear elements could be applied with the help of effective stiffness and equivalent damping (CEN 2008b), in this case an iterative procedure is needed, besides, the lack of knowledge on the actual cyclic behavior of the components questions the reliability of the results. Nonetheless, effective pier stiffness (∼50-65% of the uncracked stiffness) is accounted for, where concrete Young modulus of 30 GPa is assumed.

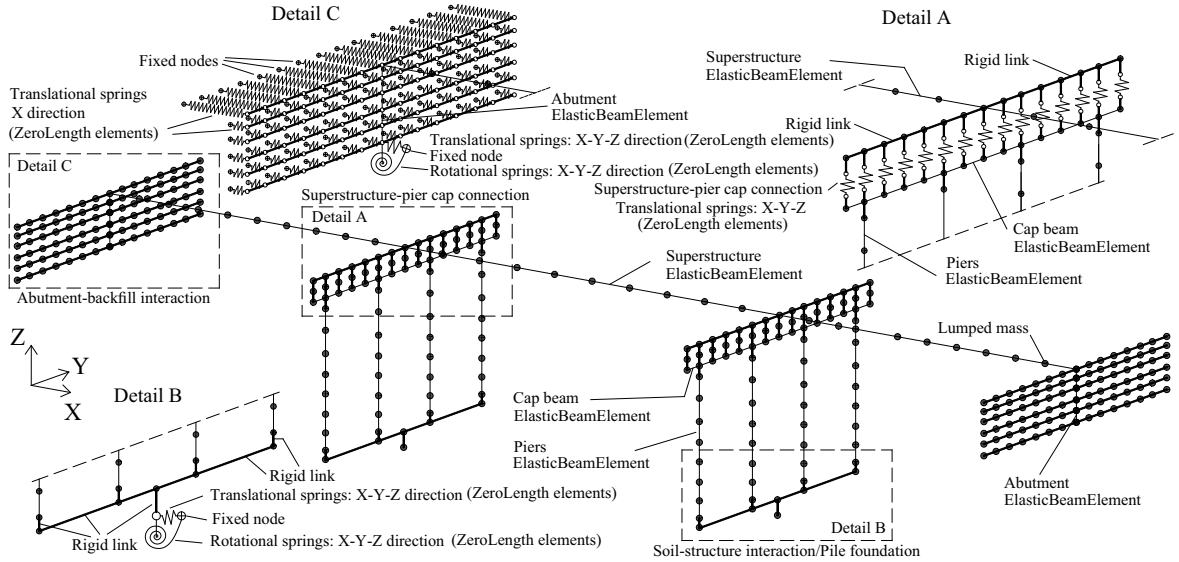


Fig. 5 Numerical model.

The monolithic joints are modeled with linear springs (Fig. 5 detail A), where a stiffness of $10^{13}$ N/m is used to model fully rigid conditions. Monolithic *Type 1* joints transfer both shear forces and bending moments, thus all DOFs are set to be fixed; while the hinged behavior of

*Type 2* joints are taken into account by assigning fixed condition to three translational ($u_x$, $u_y$, $u_z$) and two rotational DOFs ($\phi_x$, $\phi_z$) only.

The dynamic impedance of the soil-foundation system can be approximated through assemblies of springs, dashpots and fictitious masses (Wolf (1985); Ceresa *et al.* (2012)). In this study, a conservative approach is followed, both radiation and material damping of the soil is neglected, while linear springs are used to take into consideration the translational and flexural stiffness of the pile foundation (Fig. 5 detail B). The vertical stiffness of an individual pile is determined as the initial stiffness of a simplified tri-linear behavior, representing the combined behavior of skin friction and tip resistance; the horizontal stiffness is estimated according to EC8-5 Annex C (CEN 2009a). The translational and rotational stiffness of the foundations are calculated directly from the vertical and horizontal stiffness of the individual piles considering the actual layout of the pile foundation system.

Since PMG and slab bridges are built with monolithic joints, the seismic resistance is provided by both piers and abutments. In this case, the use of lower and upper bound estimates of the soil stiffness is recommended to obtain conservative demands for both the internal forces and deformations. Table 2 illustrates representative stiffness values considering the Young modulus of the soil as either 10 MPa (lower) or 100 MPa (upper) (typical range from soft to stiff clay and from loose to compact sand).

Table 2 Stiffness values of the foundation springs. $k_x$, $k_y$ and $k_z$ denote translational stiffness along the x, y and z axis (see Fig. 5); while $k_{xx}$, $k_{yy}$, $k_{zz}$ represent rotational stiffness values about the same axes, respectively.

| | | Abutment | | | | | | Pier | | | | | |
|---|---|---|---|---|---|---|---|---|---|---|---|---|---|
| Span length | Stiffness estimation | $k_x$ | $k_y$ | $k_z$ | $k_{xx}$ | $k_{yy}$ | $k_{zz}$ | $k_x$ | $k_y$ | $k_z$ | $k_{xx}$ | $k_{yy}$ | $k_{zz}$ |
| | | $10^9$ N/m | | | $10^9$ Nm/rad | | | $10^9$ N/m | | | $10^9$ Nm/rad | | |
| L15 | Lower | 0.28 | 0.28 | 0.56 | 11.44 | 1.99 | | 0.56 | 0.56 | 1.13 | 22.88 | 5.61 | |
| | Upper | 1.72 | 1.72 | 0.56 | 12.99 | 3.54 | | 3.43 | 3.43 | 1.13 | 25.99 | 8.71 | |
| L30 | Lower | 0.28 | 0.28 | 0.94 | 17.74 | 1.99 | $10^4$ | 0.56 | 0.56 | 1.88 | 35.48 | 6.68 | $10^4$ |
| | Upper | 1.72 | 1.72 | 0.94 | 19.29 | 3.54 | | 3.43 | 3.43 | 1.88 | 38.59 | 9.79 | |

The backfill soil under compression provides extra support in addition to the stiffness of the abutment. Its influence on the seismic response can be dominant in the longitudinal direction. As part of the Caltrans seismic research program, full-scale abutment field experiments were conducted (Maroney 1995). The test results showed hyperbolic force-deformation behavior of the abutment-backfill soil system subjected to monotonic longitudinal loading. This behavior is approximated in the model with linear springs (due to the linear nature of the analysis method) using the initial stiffness of the backfill soil. One end of the springs is attached to the nodes of a rigid grid modeling the surface of the abutment; the other end is attached to fixed nodes (Fig. 5 detail C). The initial stiffness of the hyperbolic curve is calculated per Caltrans (2013) from an initial stiffness value ($K_i$) determined for the entire width ($W$) of the bridge. The stiffness is adjusted to a typical backwall height ($H$=2m) and lumped to the abutment surface nodes proportionally to the corresponding areas ($A$):

$$K_0 = (K_i \cdot W \cdot (H/1.7m))/A \tag{1}$$

MMRSA cannot take into account that the backfill soil works only in compression, it

assigns the same initial stiffness in the tension zone as well. The examined bridges have both longitudinal and transverse axes of symmetry, thus the longitudinal vibration mode with movements toward one abutment is identical to the one moving toward the other abutment. For this reason, during linear MMRSA spring elements are applied at only one of the abutments to model the effect of the backfill soil only in compression. The simplified modeling of soil-structure interactions is sufficient for present preliminary study, more advanced and detailed modeling can be found in (Simon and Vigh 2016).

## 5. Results

### *5.1 Modal analysis*

Typical vibration modes of different PMG configurations are illustrated in Fig. 6a-d. The modal analysis results show the high stiffness and thus low fundamental periods of these structures. In the case of shorter, less flexible bridges (see shorter span lengths in Fig. 6e), the fundamental period is often lower than the $T_c$ corner period (see Fig. 4), thus it falls onto the plateau of the applied response spectrum. This indicates that high base shear forces are expected and that these bridges are possibly vulnerable against seismic actions.

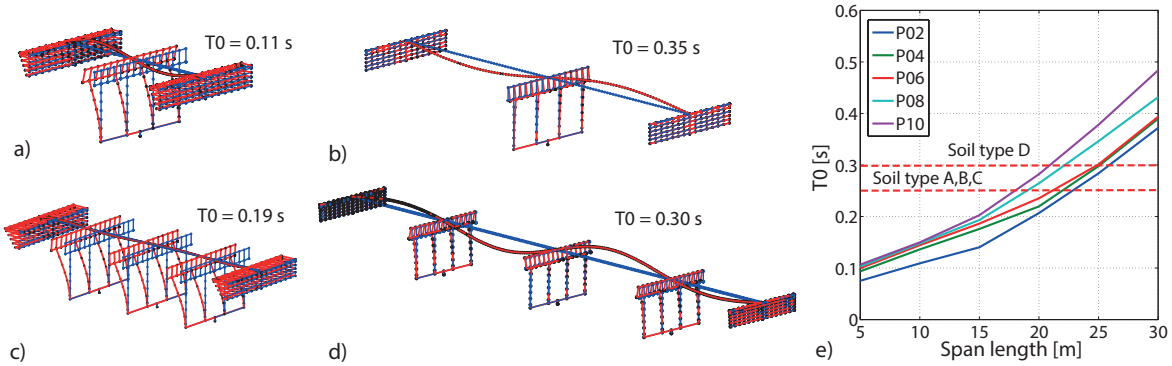


Fig. 6 First vibration modes and fundamental periods for different typical layouts of W14P06 bridges. a) S2L10; b) S2L25; c) S4L10; d) S4L25. e) Fundamental periods for W14S4 bridges ($T_C$ periods: *red dashed line*).

Fig. 7a shows typical vibration modes of the W08S4L30P06 slab configuration, illustrating the high level of interaction between the longitudinal and vertical vibrations; pier shear and bending also occur during vertical vibration due to the monolithic joint *Type 1*. Similarly to PMG bridges, slab bridges can also be characterized by high vibration frequencies (Fig. 7b), the fundamental periods are often on the plateau of the applied spectrum.

### *5.2 Effect of the soil-structure interaction*

Since PMG and slab bridges are built with monolithic joints, the seismic resistance is provided by both piers and abutments, thus the soil-structure interaction (SSI) can significantly influence the seismic behavior. In this case, the use of upper and lower bound estimates of the soil stiffness (see Table 2) is recommended to obtain conservative demands

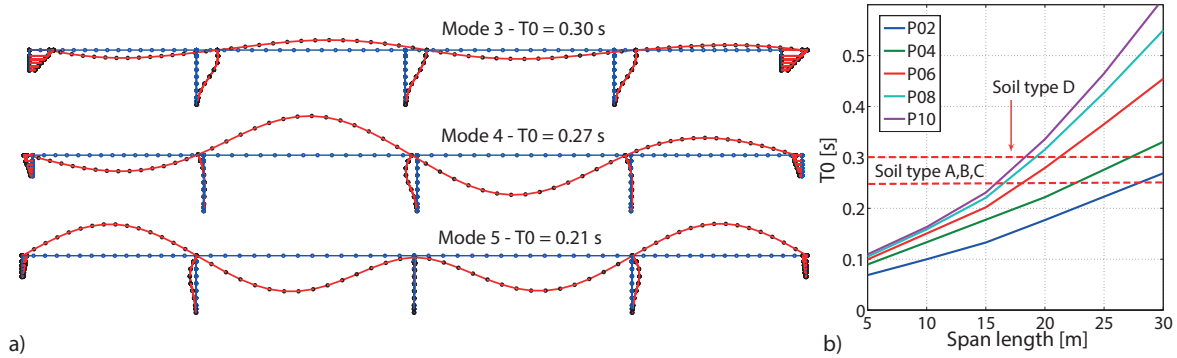


Fig. 7 a) Typical vibration modes and fundamental periods for the W08S4P06L30 configuration. b) Fundamental periods of W14S4 configurations ($T_C$ periods: *red dashed line*).

for each bridge component. The effect of the backfill soil is also investigated with two different stiffness values ($K_i$ = 28.7 kN/mm/m and 14.35 kN/mm/m) per Caltrans (2013). Three cases are examined: in each case one of the three components (backfill soil - *100*, abutment foundation - *010*, pier foundation - *001*) is characterized with its higher, while the other two with their lower stiffness values. In Table 3 and 4 representative results are illustrated for two different layouts for PMG and slab bridges, respectively.

Table 3 Sensitivity of MMRSA results to different SSI stiffness. P06L20 PMG bridges: a) W08S2; b) W20S4. Δ denotes the relative difference between maximum and minimum values in %.

| a) | Pier internal forces | | | | Abutment joint | | Pier joint | | Backfill | Disp. | |
|---|---|---|---|---|---|---|---|---|---|---|---|
| Code | $V_x$ [kN] | $V_y$ [kN] | $M_x$ [kNm] | $M_y$ [kNm] | $F_x$ [kN] | $F_y$ [kN] | $F_x$ [kN] | $F_y$ [kN] | $\sigma$ [kPa] | $d_x$ [mm] | $d_y$ [mm] |
| *100* | 25 | 153 | 456 | 122 | 2218 | 1370 | 30 | 387 | 63 | 3 | 6 |
| *010* | 23 | 125 | 368 | 103 | 2295 | 1355 | 17 | 293 | 26 | 3 | 5 |
| *001* | 32 | 172 | 514 | 163 | 2202 | 1336 | 46 | 440 | 38 | 4 | 6 |
| Δ % | 39 | 38 | 40 | 58 | 4 | 3 | 167 | 50 | 145 | 56 | 25 |
| b) | Pier internal forces | | | | Abutment joint | | Pier joint | | Backfill | Disp. | |
| Code | $V_x$ [kN] | $V_y$ [kN] | $M_x$ [kNm] | $M_y$ [kNm] | $F_x$ [kN] | $F_y$ [kN] | $F_x$ [kN] | $F_y$ [kN] | $\sigma$ [kPa] | $d_x$ [mm] | $d_y$ [mm] |
| *100* | 59 | 250 | 745 | 310 | 8398 | 4756 | 281 | 1164 | 121 | 7 | 7 |
| *010* | 45 | 192 | 571 | 204 | 8082 | 4802 | 213 | 894 | 49 | 5 | 6 |
| *001* | 70 | 261 | 781 | 377 | 8303 | 4621 | 340 | 1217 | 76 | 8 | 7 |
| Δ % | 57 | 36 | 37 | 85 | 4 | 4 | 59 | 36 | 147 | 64 | 20 |

Conservative pier internal forces and pier joint shear forces are obtained considering the pier foundation as the stiffest element of the SSI (code: *001*). The same behavior can be observed in case of the abutment-backfill soil system. The increased stiffness of these components (code: *100* or *010*) can slightly affect the abutment joint shear forces; while the passive earth pressure is significantly dependent on the stiffness of the backfill soil (code: *100*). Observing the girder displacements, both longitudinal and transverse movements are controlled by the stiffness of the abutment foundation (code: *010*). The results for slab bridges are similar to the ones observed in case of PMG bridges, however note that pier internal forces are increased compared to PMG bridges with the same configurations. As

Table 4 Sensitivity of MMRSA results to different SSI stiffness. P06L20 slab bridges: a) W08S2; b) W20S4. $\Delta$ denotes the relative difference between maximum and minimum values in %.

| a) | Pier internal forces | | | | Abutment joint | | Pier joint | | Backfill | Disp. | |
|---|---|---|---|---|---|---|---|---|---|---|---|
| Code | $V_x$ [kN] | $V_y$ [kN] | $M_x$ [kNm] | $M_y$ [kNm] | $F_x$ [kN] | $F_y$ [kN] | $F_x$ [kN] | $F_y$ [kN] | $\sigma$ [kPa] | $d_x$ [mm] | $d_y$ [mm] |
| *100* | 89 | 221 | 661 | 257 | 3110 | 1629 | 200 | 577 | 85 | 4 | 8 |
| *010* | 64 | 189 | 562 | 178 | 2905 | 1602 | 128 | 478 | 32 | 3 | 7 |
| *001* | 106 | 247 | 738 | 315 | 2889 | 1585 | 253 | 654 | 48 | 5 | 8 |
| $\Delta$ % | 67 | 30 | 31 | 77 | 8 | 3 | 98 | 37 | 166 | 65 | 19 |
| b) | Pier internal forces | | | | Abutment joint | | Pier joint | | Backfill | Disp. | |
| Code | $V_x$ [kN] | $V_y$ [kN] | $M_x$ [kNm] | $M_y$ [kNm] | $F_x$ [kN] | $F_y$ [kN] | $F_x$ [kN] | $F_y$ [kN] | $\sigma$ [kPa] | $d_x$ [mm] | $d_y$ [mm] |
| *100* | 269 | 440 | 1311 | 752 | 13244 | 8316 | 815 | 1449 | 192 | 10 | 11 |
| *010* | 231 | 321 | 955 | 635 | 12977 | 8669 | 672 | 1034 | 80 | 8 | 9 |
| *001* | 295 | 461 | 1375 | 842 | 11160 | 8202 | 916 | 1524 | 103 | 11 | 11 |
| 6 | 247 | 738 | 315 | 2889 | 1585 | 253 | 654 | 48 | 5 | 8 | |
| $\Delta$ % | 27 | 43 | 44 | 33 | 18 | 6 | 36 | 47 | 140 | 32 | 22 |

confirmed by Table 3 and 4, using non-conservative variation may lead to ∼60% underestimation of specific demands. Therefore, in this study analyses are carried out with all the three variations to calculate conservative results for each component.

### 5.3 Calculated demands

#### 5.3.1 Superstructure

In Fig. 8b vertical girder bending moments of the W14S4P06L25 PMG configuration are illustrated (note that seismic demands obtained with MMRSA are always positive due to the combination of modal responses, however negative signed values are also valid because of the bi-directional nature of earthquakes). The moments from dead load are dominantly sagging due to the composite construction technology (considerable dead load is carried by the simply supported girders, since continuity is created after the hardening process of the concrete slab). A significant contribution can be observed from the longitudinal vibration (EQX) compared to the vertical one (EQZ). This can be explained as follows. Horizontal forces are transferred with eccentricity from the substructure. The longitudinal movement of the piers can develop only if the girders are bent (Fig. 8a). The high stiffness of the whole system implies significant bending moments; besides, the intensity of the horizontal ground motion is usually higher.

As for slab bridges, vertical bending moments illustrated in Fig. 9a shows that the contribution of the longitudinal vibration (EQX) is still as significant as the vertical one (EQZ). However, the total seismic effect is negligible compared to the dead load in this case.

Evaluation of the superstructure is carried out as follows. Even though the girders are not designed for seismic action, they should withstand the demands in Ultimate Limit State (ULS). Internal forces are determined both in ULS and in seismic combination (EQ). In Fig. 8c, ratios of maximum bending moments of PMG bridges, calculated in accordance with the former Hungarian standard ÚT (2004) and with EC0 (CEN 2011) are shown. The two standards differ in the partial factor of the dead load (1.1 and 1.35 in ÚT and EC,

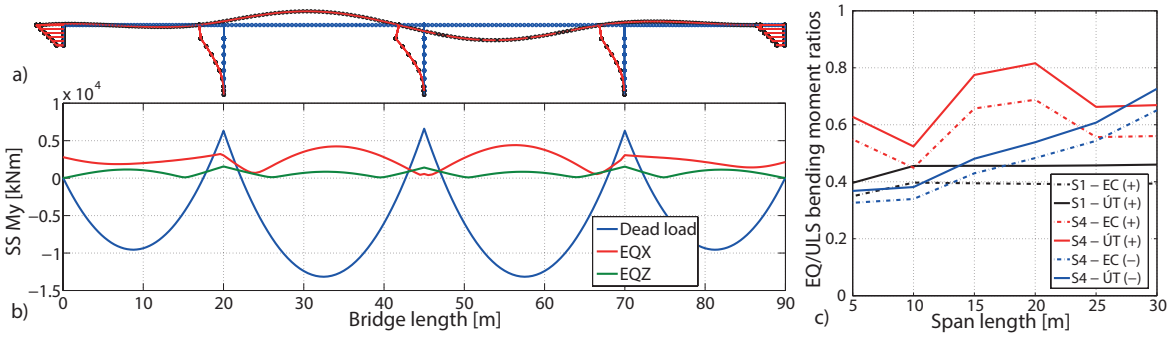


Fig. 8 a) Dominant vibration mode in the longitudinal direction. b) Vertical superstructure (SS) bending moments ($M_y$) of the W14S4P06L25 PMG configuration. c) EQ/ULS $M_y$ ratios for W14P06 PMG bridges.

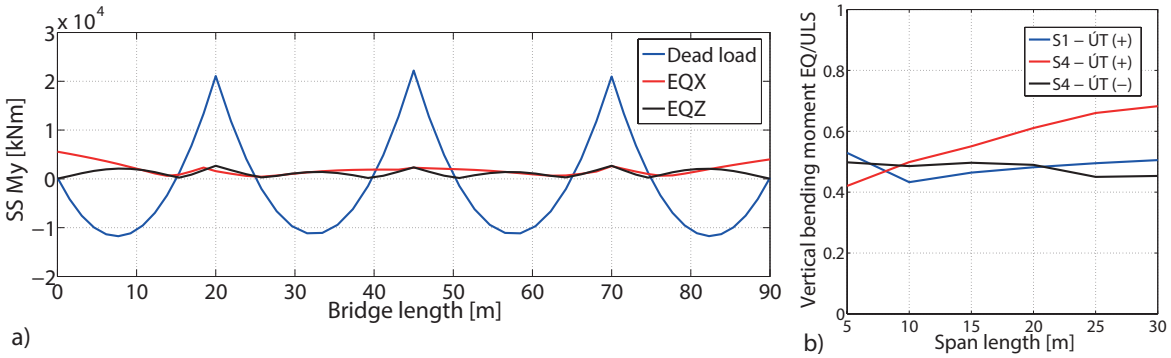


Fig. 9 a) Vertical bending moments (My) of the superstructure (W14S4P06L25 slab configuration). b) Ratios of vertical bending moments calculated in EQ and ULS for W14P06 slab bridges.

respectively) leading to a significant difference in the superstructure capacity. The induced additional safety per EC results in higher capacity and better seismic performance. The EQ/ULS ratios indicate that single span bridges are less vulnerable; and even for multi-span bridges the critical ratio of 1.0 (failure of the girders) for either sagging (+) or hogging (-) moments is not reached. The low vilnerability of slab bridges can also be confirmed, Fig. 9b shows that the EQ/ULS ratios (calculated per ÚT) remain under 0.7.

Transverse bending moments of the superstructure may be higher than those from ULS, however the flexural capacity is still an order of magnitude greater, failure is not expected. For instance, the compressive stress in the external concrete fiber is around 2-5 MPa in case of both PMG and slab bridges.

### *5.3.2 Monolithic joints*

In Fig. 10a-d resultant joint shear forces are shown. Increasing demands with increasing span length is a general tendency due to the higher applied mass. Shear forces are higher at the superstructure-abutment joint as a result of the relatively high stiffness of the abutment-backfill soil system. At the abutment joint (Fig. 10a), increase is observed at shorter piers

(<4 m), while the tendency is reversed at the pier joint (Fig. 10b). The effect of the deck width is illustrated in Fig. 10c showing that the results are nearly the same for 14 m and 20 m width, while slightly increased demands are obtained for 8 m.

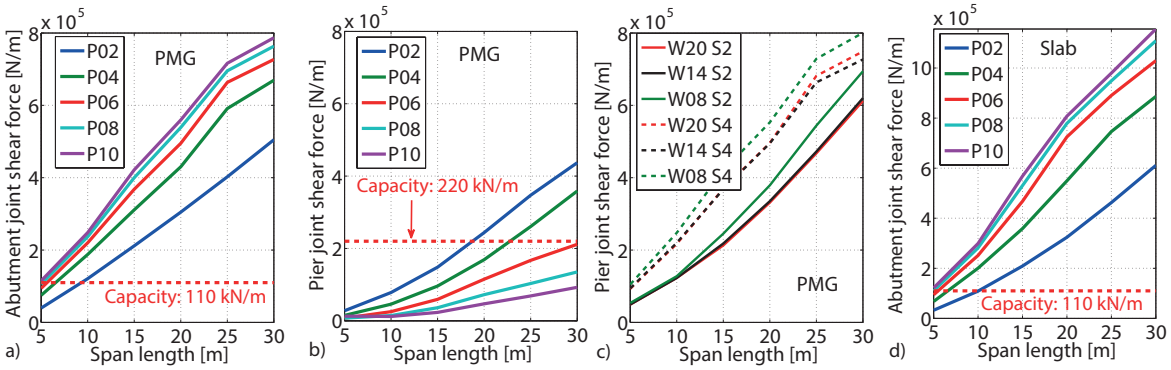


Fig. 10 Resultant joint shear forces of (normalized to deck width): a) at the abutment (W14S4 PMG configurations); b) at the pier (W14S4 PMG configurations); c) for different deck widths (PMG bridges); d) at the abutment (W14S4 slab bridges)

To evaluate critical configurations, the shear resistance of the joints ($R_u$) is determined with the formula presented in (Psycharis and Mouzakis 2012):

$$R_u = 1.1 \cdot n \cdot D^2 \cdot \sqrt{f_{cd} \cdot f_{sd}}/\gamma_R \tag{2}$$

where $n$, $D$ and $f_{sd}$ are the number, diameter and design strength of the rebars; $f_{cd}$ is the design strength of the concrete and $\gamma_R$ is the safety factor of 1.3. A conservative estimation considering C20/30 concrete and S500B rebars lead to a normalized resistance of ~110 kN/m at the abutment (with $\phi$16/150) and ~220 kN/m at the piers (with 2$\phi$16/150), in case of PMG bridges. The resistance at the abutment is definitely insufficient even for shorter spans. The lower demands and the higher resistance of the pier joint lead to a lower vulnerability (critical only at shorter piers). Note, however, that after a possible failure of the abutment joint, redistribution of the forces may risk the failure of this component as well.

Normalized abutment joint shear forces (Fig. 10d) indicate that this component may be critical for slab bridges as well. Using Eq.(2) to calculate the resistance of a typical joint with $\phi$16/150 shear reinforcement results in ~110 kN/m shear capacity showing that there is a high probability that this component fails even in case of shorter spans. The deck to pier joints are less vulnerable due to the lower shear forces, besides, it can be shown that pier shear failure is much more likely to occur prior to the failure of the monolithic joint. For instance, if a typical slab bridge is considered (W14S4P06L25), the shear forces associated with cracking of the joint is two times larger than the pier shear resistance.

### 5.3.3 Piers

Results for the PMG piers are depicted in Fig. 11a-c. Demands are lower in the longitudinal direction which stems from the longitudinal support provided by the high stiffness of the abutment and the backfill soil. The longitudinal shear forces ($V_x$), the corresponding $M_y$

bending moments and the transverse shear forces ($V_y$) have the same tendency (Fig. 11a) of being increased for shorter piers. However, in Fig. 11b, the maximum values of transverse bending moments ($M_x$) do not correspond to the lowest 2 m pier height, instead, a peak can be observed at 4 m. The pier height does not only influence the relative stiffness and thus the transferred lateral forces, but also the lever arm of these forces. The pier should be high enough to minimize the developing seismic shear forces in a way that the governing bending moments are decreased as well.

The required shear reinforcement ($A_w/s_w$) and the flexural DC ratio are calculated per EC2-2 (CEN 2009b) and EC8-2:

$$A_w/s_w = \gamma_{Bd} \cdot V_{Ed}/(z \cdot f_{wd} \cdot cot\theta) \tag{3}$$

$$DC = (M_{xEd}/M_{xRd})^a + (M_{yEd}/M_{yRd})^a \tag{4}$$

where $\gamma_{Bd}$ is a partial factor of 1.25 for brittle failure; $V_{Ed}$ is the resultant shear force; $z$ is the lever arm of internal forces; $f_{wd}$ is the design strength of the stirrups; $\theta$ is the angle of the concrete compression strut; $M_{xEd}$, $M_{yEd}$ and $M_{xEd}$, $M_{yRd}$ are the design moments and flexural resistance in each direction and the exponent $a$ takes into account the normal force in the element. Typical cross-section and material properties (0.6x0.9 m cross section; $\phi$12/150 stirrups (~1500 mm$^2$/m); ~1% longitudinal reinforcement ratio (16$\phi$20); S500B steel and conservative concrete grade C20/30) are used for the calculations. According to Fig.11c short piers show high vulnerability against shear forces (maximum applicable span length is <10 m), while flexural behavior is inadequate for higher piers (but the span length can be much longer <17 m in this case).

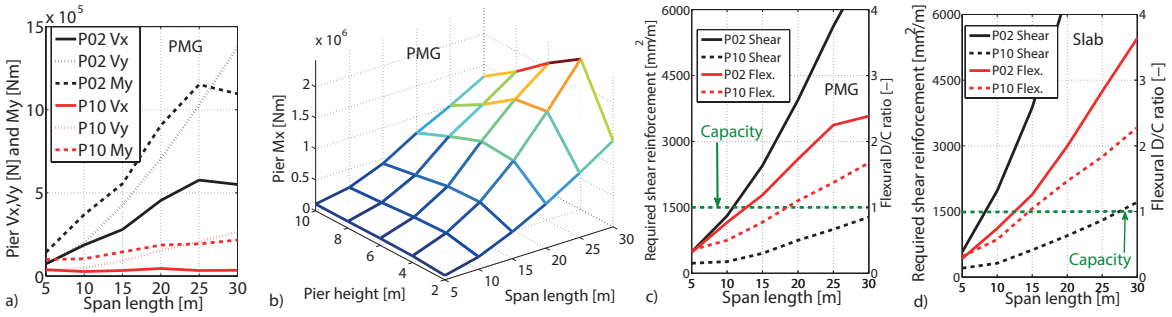


Fig. 11 Results for W14S4 configurations: a) pier shear forces ($V_x$,$V_y$) and vertical bending moments ($M_y$) (PMG); b) pier transverse bending moments ($M_x$) (PMG). Required shear reinforcement and flexural DC ratio of the pier: c) PMG bridges; d) slab bridges.

Slab bridge piers show higher vulnerability than PMG bridges against shear forces and flexural failure as well (Fig. 11d). The maximum applicable span length for short piers is under 8 m, for instance.

### *5.3.4 Piles*

The pile foundation is incorporated in the model with simple integrated springs. Detailed analysis of the individual piles is out of scope in this study, however forces transferred to

the pile head can be calculated using the foundation layout and the reaction forces. Pile normal forces are calculated to estimate whether compressive resistance failure occurs. The typical pile resistance is around 2000-2500 kN; therefore Fig. 12a-b confirm that failure is not expected except for slab bridges with extremely short piers and long spans, which is a rare configuration.

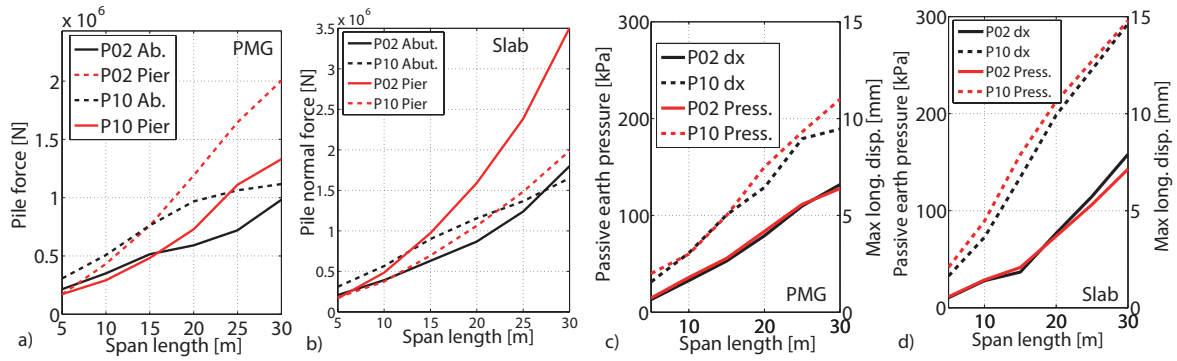


Fig. 12 Results for W14S4 configurations. Pile normal forces: a) PMG bridges; b) slab bridges. Maximum earth pressure and maximum longitudinal displacements: c) PMG bridges, d) slab bridges.

### 5.3.5 Abutment and backfill soil

Two other components, the abutment and backfill soil demands are shown in Fig. 12c-d. The abutments are considered as rigid blocks, therefore only global stability failure is taken into consideration. Demands are determined as the maximum longitudinal displacement that can possibly cause stability failure, while the backfill soil demands are measured with the maximum passive earth pressure. These demands are in high correlation, since passive earth pressure is caused by the longitudinal movements of the abutment. It can be concluded that the probability of failure is low. Passive earth pressure never reaches ∼430 kPa (ultimate failure threshold per Caltrans), while the displacements are always under 30 mm (recommended limit for bridges of importance class III per EC8-2).

### 5.4 Critical components and layouts

To highlight critical components and layouts, maximum acceptable PGA (MAPGA; DC ratio is divided by the applied PGA value) is calculated for each component of each configuration. The capacities of the components are the ones presented in the previous subsections. Fig. 13 presents the dependency of MAPGA on the pier height and deck width in case of PMG bridges. The pier height highly influences the pier internal forces (especially shear), thus the MAPGA values as well (Fig. 13a-b). As confirmed by Fig. 13c-d, the results are less sensitive to the deck width, pier height and the length of the superstructure are far more important structural attributes.

It is assumed that the failure of one component can initiate the failure of the whole system (series system). It is important to understand which component is the most vulnerable for different layouts. In Fig. 14, MAPGA results for the most vulnerable components are illustrated for W14S3 PMG configurations. High vulnerability of the abutment joint is

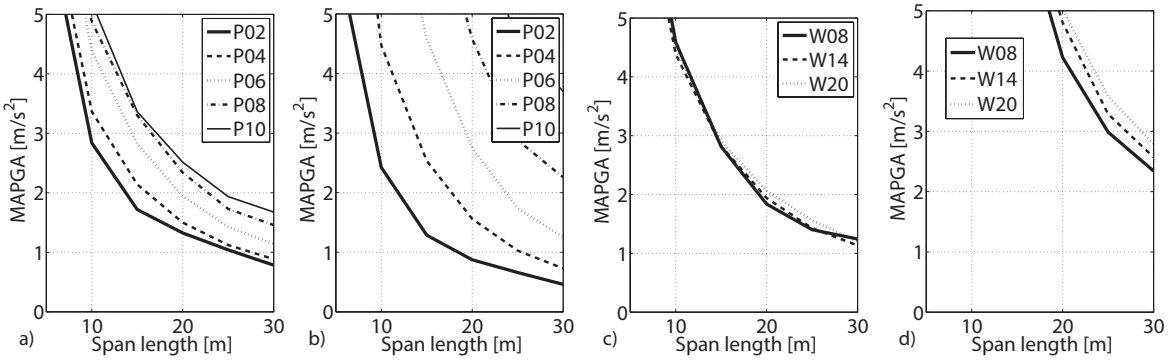


Fig. 13 MAPGA values of S3 PMG bridges. Different pier heights (W14): a) pier bending; b) pier shear. Different widths (P06): d) pier bending; e) pier pile compression. Typical moderate PGA range: 1-2 m/s$^2$.

confirmed, this component is the most critical for every configuration. Failure of the pier is characterized by shear or flexural failure for shorter or higher piers, respectively. Note that flexural capacity can be characterized with at least a limited ductile behavior. This indicates the sensitivity of piers to shear forces for pier heights (5-6 m) typically used in case of highway bridges.

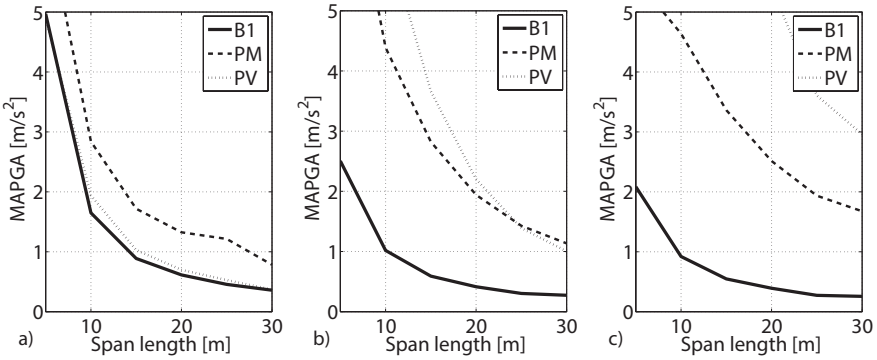


Fig. 14 Critical components for W14S3 PMG configurations: a) P02; b) P06; c) P10. (B1-abutment joint; PM – pier flexural failure; PV – pier shear failure). Typical moderate PGA range: 1-2 m/s$^2$.

MAPGA values are calculated for slab bridges as well. The dependencies on the deck width and pier height are similar to those presented in Fig. 13 in case of PMG bridges, while the critical components are also identical for the same configurations. However, pier internal forces are generally higher in case of slab bridges for the same arrangement due to the different monolithic joint *Type 1*, transferring not only shear forces but also bending moments. Besides, the mass of the slab bridges is also higher causing higher seismic demands. Table 5 illustrates the differences in MAPGA values related to pier flexural and shear failure of W14S4 bridges. Worse performance can be observed for both bridge classes if the piers are shorter and the spans are longer. Note the better performance of PMG bridges for a typical highway overpass configuration (P06 and L20-25).

Table 5 MAPGA values for pier flexural and shear failure of W14S4 bridges.

| Slab | | | | | | PMG | | | | | | Pier height [m] | |
|---|---|---|---|---|---|---|---|---|---|---|---|---|---|
| 6.9 | 2.6 | 1.5 | 1.0 | 0.7 | 0.5 | 6.2 | 2.5 | 1.6 | 1.1 | 0.9 | 0.8 | 2 | Flexural |
| 5.1 | 1.9 | 1.0 | 0.6 | 0.5 | 0.4 | 5.8 | 2.7 | 1.6 | 1.2 | 0.8 | 0.7 | 4 | |
| 5.6 | 2.3 | 1.2 | 0.8 | 0.6 | 0.5 | 6.7 | 3.4 | 2.0 | 1.3 | 0.9 | 0.8 | 6 | |
| 6.3 | 2.9 | 1.5 | 1.1 | 0.8 | 0.7 | 6.8 | 3.9 | 2.3 | 1.5 | 1.2 | 1.0 | 8 | |
| 6.2 | 3.4 | 1.9 | 1.3 | 1.1 | 0.9 | 5.5 | 3.9 | 2.5 | 1.8 | 1.4 | 1.2 | 10 | |
| 3.9 | 1.1 | 0.6 | 0.3 | 0.2 | 0.2 | 4.6 | 1.7 | 0.9 | 0.6 | 0.4 | 0.3 | 2 | Shear |
| 5.2 | 1.7 | 0.8 | 0.4 | 0.3 | 0.2 | 7.2 | 2.8 | 1.4 | 0.8 | 0.5 | 0.4 | 4 | |
| 7.9 | 3.1 | 1.4 | 0.8 | 0.6 | 0.5 | 10.3 | 4.6 | 2.2 | 1.2 | 0.8 | 0.7 | 6 | |
| 10.6 | 5.0 | 2.3 | 1.4 | 1.0 | 0.8 | 12.3 | 6.8 | 3.5 | 1.9 | 1.4 | 1.1 | 8 | |
| 10.9 | 7.1 | 3.6 | 2.4 | 1.7 | 1.3 | 9.8 | 8.4 | 5.0 | 3.0 | 2.2 | 1.8 | 10 | |
| 5 | 10 | 15 | 20 | 25 | 30 | 5 | 10 | 15 | 20 | 25 | 30 | Span length [m] | Component |

## 6. Nationwide seismic performance evaluation

A possible application of the parametric results is illustrated through the example of a nationwide seismic performance evaluation in Hungary as follows:

1. Essential parameters of a specific bridge are obtained from the Hungarian road bridge database (HTA 2016) (bridges without sufficient input parameters are excluded).
2. MAPGA values are determined with linear interpolation on the parametric results for each structural component.
3. MAPGA values are modified with a factor reflecting bridge condition (the existing bridge database employs a 5 level scale with 1 being excellent condition and 5 being extensive damages; from condition 1 to 5 a factor of 1.0-0.6 is applied).
4. PGA value for the bridge site is determined using the seismic zonation map of Hungary (Tóth *et al.* 2006).
5. DC ratio of each component is calculated comparing the PGA and the corresponding MAPGA.

To illustrate the utilization of each bridge component regarding all the examined bridges, empirical cumulative distributions (representing non-exceedance) of the component DC ratios are created (Fig. 15). For example, the B1 curve in Fig. 15a shows that the abutment monolithic joint is critical for ∼20% of single span bridges, while the PV curve in Fig. 15b indicates that ∼30% of the multi-span bridges have inadequate pier shear resistance.

In case of single span bridges only the abutment joint is critical. In 22% of the observed 1313 bridges, there is a possibility that this component fails (Table 6). The percentage is lower for slab bridges, for they are often constructed for shorter spans. Failure of this component is highly probable for multi-span bridges as well, more than 90% of the bridges have inadequately detailed abutment joint.

The joint failure does not necessary cause progressive collapse in case of multi-span bridges; pier failure is far more dangerous. Table 6 also shows the relative number of bridges where collapse occurs either with pier flexural or shear failure. According to Table 6, pier

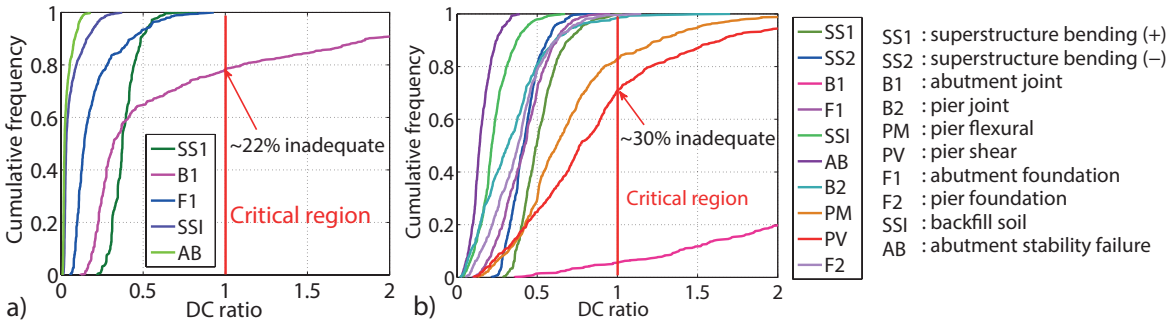


Fig. 15 Critical bridge components of a) single and; b) multi-span bridges.

Table 6 Relative number of critical bridge components.

| | Single span bridges | | Multi span bridges | | | |
|---|---|---|---|---|---|---|
| | Abutment joint | Total number | Abutment joint | Pier flexural | Pier shear | Total number |
| PMG | 29% | 758 | 94% | 1% | 22% | 602 |
| Slab | 12% | 555 | 96% | 4% | 51% | 166 |
| ALL | 22% | 1313 | 95% | 2% | 28% | 768 |

shear failure is critical for the most commonly used typical highway overpass layout (P06 and L20-25). This is reflected in the results: pier shear failure is more likely to occur regarding the whole bridge stock. Note also that a significant portion of slab bridges may suffer pier failure even though they are usually constructed with shorter spans. It should be emphasized, however, that these results are obtained with conservative assumptions (both for capacities and demands), thus the number of critical structures may be lower in reality.

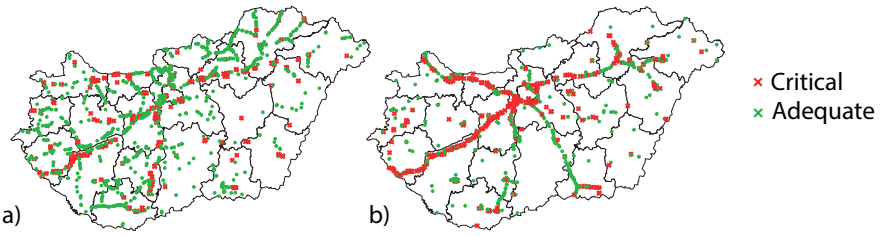


Fig. 16 Critical bridges. a) Single span - abutment joint failure. b) Multi span - pier failure.

In Fig. 16, single span bridges with possible abutment joint and multi-span bridges with pier failure (causing progressive collapse) are illustrated. These maps are useful tools to identify critical bridges and to select regions of interest for a possible retrofitting project.

## 7. Conclusions

Precast multi-girder and slab bridges have a significant contribution to typical bridge inventories. Most bridges were non-seismically designed in several moderate seismic areas; the seismic behavior of these structures is not known. A parametric seismic analysis is carried out to examine the seismic behavior and to determine possible critical components

and layouts. The following conclusions are drawn from the results:

- Modal analysis confirms that these structures are relatively stiff, the fundamental period often falls onto the plateau of the applied response spectrum.
- Investigation of the effect of the soil-structure interaction concludes that internal forces and displacements are highly dependent on the relative stiffness values of the SSI components. The analysis should be carried out taking into account conservative stiffness combinations for each bridge component.
- Due to the integral construction, longitudinal movements of the piers and abutments cause vertical bending in the superstructure; relatively high bending moments develop that are comparable with (or even higher than) those caused by vertical vibration. This phenomenon is more dominant if the span number is even (e.g. 4-span bridges). However, it is also shown that the superstructure is likely to be adequate even though it is designed only for ULS combinations.
- Seismic demands are increasing with bridge length, while monolithic joint shear forces, pier demands highly, foundation normal forces moderately, abutment and backfill-soil demands slightly depend on pier height. The deck width is a far less important structural attribute regarding the seismic behavior.
- The failure of the abutment and the backfill soil is not expected; it is also shown that pile compressive resistance is adequate in case of typical bridge layouts.
- Single-span bridges are less vulnerable, however failure of the abutment monolithic joint may occur.
- Longer multi-span bridges are more vulnerable, the most critical component is the abutment monolithic joint. Note, however, that progressive collapse is initiated with the failure of the piers, which can be characterized as expected: shorter piers suffer shear, while higher piers suffer flexural failure.
- Piers can be characterized with at least a limited flexural ductility, thus the results highlight the high vulnerability of piers to brittle shear failure.
- Observing multi-span configurations in a typical bridge inventory, it is found that 30% of the bridges may suffer pier failure, which implies significant economic consequences.
- The results related to the high vulnerability of the piers to brittle shear failure suggest a more in deep investigation, with more refined modelling strategies (Kagermanov and Ceresa (2016); Ceresa *et al.* (2009)) taking into account the flexure-shear interaction in the seismic response of the piers.

Although the accuracy of the adopted method is insufficient for estimating the extent of damage, it provides a realistic basis for assessing the overall seismic performance. Such a preliminary parametric analysis can allow us to sketch the most vulnerable components and layouts, therefore to improve the knowledge on and the prevention of the seismic risk at a national scale. The results enable the authorities to decide about future actions: e.g.

to elaborate risk prevention plans and retrofit priorizations. The illustrated preliminary parametric seismic analysis approach can be efficiently used for: 1) further detailed seismic assessment and risk based seismic analysis; 2) retrofit planning for the critical bridges; 3) development of design concepts of newly built structures in moderate seismicity areas.

## Acknowledgements

This paper was supported by the János Bolyai Research Scholarship of the Hungarian Academy of Sciences. The authors highly appreciate the help of the members of the Hungarian Transport Administration, who provided the bridge database and gave instructions about its structure and application.

## References

Akiyama, H. and Kajikawa, Y. (2008), *Fundamentally structural characteristics of integral bridges*, Thesis, Graduate School of Natural Science and Technology, Kanazawa University, Japan.

Avşar, Ö., Yakut, A. and Caner, A. (2011), "Analytical Fragility Curves for Ordinary Highway Bridges in Turkey", *Earthquake Spectra*, **27**(4), 971-–996. DOI: 10.1193/1.3651349.

Billah, A.H.M.M. and Alam, M.S. (2015), "Seismic fragility assessment of highway bridges: a state-of-the-art review", *Structure and Infrastructure Engineering*, **11**(6), 1-29. DOI: 10.1080/15732479.2014.912243.

Borzi, B., Ceresa, P., Faravelli, M., Fiorini, E. and Onida, M. (2013), "Seismic Risk Assessment of Italian School Buildings", *Computational Methods in Applied Sciences*, **30**(1), 317–344. DOI: 10.1007/978-94-007-6573-3_16.

Borzi, B., Ceresa, P., Franchin, P., Noto, F., Calvi, G.M. and Pinto, P.E. (2015), "Seismic Vulnerability of the Italian Roadway bridge stock", *Earthquake Spectra*, **31**(4), 2137–2161. DOI: 10.1193/070413EQS190M.

BSSC (2009), *NEHRP Recommended Seismic Provisions for New Buildings and Other Structures (FEMA P-750)*, Building Seismic Safety Council (BSSC), Washington D.C.

Caltrans (2013), *Caltrans Seismic Design Criteria*, California Department of Transportation, Sacramento, CA, Version 1.7.

CEN (2008a), *MSZ EN 1998-1 Eurocode 8: Design of structures for earthquake resistance. Part 1: General rules, seismic actions and rules for buildings*, CEN.

CEN (2008b), *MSZ EN 1998-2 Eurocode 8: Design of structures for earthquake resistance. Part 2: Bridges*, CEN.

CEN (2009a), *MSZ EN 1998-5 Eurocode 8: Design of structures for earthquake resistance. Part 5: Foundations, retaining structures and geotechnical aspects*, CEN.

CEN (2009b), *MSZ EN 1992-2 Eurocode 2: Design of concrete structures. Part 2: Concrete bridges. Design and detailing rules*, CEN.

CEN (2011), *MSZ EN 1990-1 Eurocode 0: Basis of structural design*, CEN.

Ceresa, P., Petrini, L., Pinho, R. and Sousa, R. (2009), "A fibre flexure-shear model for seismic analysis of RC-framed structures", *Earthquake Engineering and Structural Dynamics*, **38**(5), 565–586. DOI: 10.1002/eqe.894.

Ceresa, P., Brezzi, F., Calvi, G.M. and Pinho, R. (2012), "Analytical modelling of a large-scale

dynamic testing facility", *Earthquake Engineering and Structural Dynamics*, **41**(2), 255–277. DOI: 10.1002/eqe.1128.

Choi, E. and Jeon, J.C. (2003), "Seismic fragility of typical bridges in moderate seismic zone", *KSCE Journal of Civil Engineering*, **7**, 41–51.

Chopra, A. K. (1995), *Dynamics of structures: Theory and applications to earthquake engineering*, Englewood Cliffs, N.J: Prentice Hall.

Connal, J. (2004), "Integral abutment bridges-Australian and US practice, in *5th Austroads bridge conference*, Hobart, Australia.

Fagà, E., Ceresa, P., Nascimbene, R., Moratti, M. and Pavese, A. (2016), "Modelling curved surface sliding bearings with bilinear constitutive law: effects on the response of seismically isolated buildings", *Materials and Structures*, **49**(6), 2179–2196. DOI: 10.1617/s11527-015-0642-2.

Fennema, J., Laman, J. and Linzell, D. (2005), "Predicted and measured response of an integral abutment bridge", *Journal of Bridge Engineering*, **10**(6), 666–677.

Gilbert, A.D. (1993), "Developments in seismic prioritization of bridges in California, in *Compte rendu du 9th US-Japan Bridge Engineering Workshop*, pp. 227-240.

HTA (2016), *Integrated Bridge Database*, http://www.hidadatok.hu, Hungarian Transport Administration, Budapest, Hungary.

Kagermanov, A. and Ceresa, P. (2016), "Physically Based Cyclic Tensile Model for RC Membrane Elements", *Journal of Structural Engineering (ASCE)*, **142**(12). DOI: 10.1061/(ASCE)ST.1943-541X.0001590.

Kawashima, K. and Unjoh, S. (1990), "An inspection method of seismic vulnerability of existing highway bridges", *Structural Engineering and Earthquake Engineering*, **7**(1), 143–150.

Kibboua, A., Bechtoula, H., Mehani, Y. and Naili, M. (2014), "Vulnerability assessment of reinforced concrete bridge structures in Algiers using scenario earthquakes", *Bulletin of Earthquake Engineering* **12**(2), 807–827. DOI: 10.1007/s10518-013-9523-7.

Marchand, P., Davi, D., Schmitt, P., Thibault, C., Duval, A.M. and Criado, D (2006), "SISMOA: a simplified method to assess the seismic vulnerability of existing bridges, in *First European conference on earthquake engineering and seismology*, Geneva, Switzerland.

Maroney, B.H. (1995), *Large scale bridge abutment tests to determine stiffness and ultimate strength under seismic loading*, Ph.D. dissertation, Dept. of Civil Engineering, University of California Davis, CA.

McKenna, F., Scott, M.H. and Fenves, G.L. (2010), "Nonlinear finite-element analysis software architecture using object composition", *Journal of Computing in Civil Engineering*, **24**(1), 97–105. DOI: 10.1061/(ASCE)CP.1943-5487.0000002.

Moschonas, I.F., Kappos, A.J., Panetsos, P., Papadopoulos, V., Makarios, T. and Thanopoulos, P. (2009), "Seismic fragility curves for Greek bridges: methodology and case studies", *Bulletin of Earthquake Engineering*, **7**(2), 439–468. DOI: 10.1007/s10518-008-9077-2.

Nielson, B.G. (2005), *Analytical Fragility Curves for Highway Bridges in Moderate Seismic Zones*, PhD dissertation, School of Civil and Environmental Engineering, Georgia Institute of Technology.

OFROU (2005), *Evaluation parasismique des ponts routes*, Office Fédéral Suisse des Routes

Pinto, P.E. and Franchin, P. (2010), "Issues in the upgrade of Italian highway structures", *Journal of Earthquake Engineering*, **14**(1), 1221–1252.

Psycharis, N.I. and Mouzakis, P.H. (2012), "Shear resistance of pinned connections of precast members to monotonic and cyclic loading", *Engineering Structures*, **41**(1), 413–427. DOI:

10.1016/j.engstruct.2012.03.051.

Ramanatan, K., DesRoches, R. and Padgett, J.E. (2012), "A comparison of pre- and post-seismic design considerations in moderate seismic zones through the fragility assessment of multispan bridge classes", *Engineering Structures*, **45**, 559–573.

Simon, J. and Vigh, L.G. (2014), "Multi modal response spectrum analysis implemented in OpenSees", in *OpenSees Days Portugal*, Porto, Portugal, pp. 39-42.

Simon, J., Vigh, L. G., Horváth, A. and Pusztai, P. (2015), "Application and assessment of equivalent linear analysis method for conceptual seismic retrofit design of Háros M0 highway bridge", *Periodica Polytechnica*, **59**(2), 109–122. DOI: 10.3311/PPci.7860.

Simon, J. and Vigh, L.G. (2016), "Seismic fragility assessment of integral precast multi-span bridges in areas of moderate seismicity", *Bulletin of Earthquake Engineering*, (in press). DOI: 10.1007/s10518-016-9947-y.

Solomos, G., Pinto, A. and Dimova, S. (2008), *A review of the seismic hazard zonation in national building codes in the context of Eurocode 8*, JRC Scientific and Technical Reports.

Tóth, L., Győri, E., Mónus, P. and Zsíros, T. (2006), "Seismic hazard in the Pannonian Region. The Adria Microplate: GPS Geodesy, Tectonics, and Hazards", *Springer Verlag, NATO ARW Series*, **61**(1), 369–384.

ÚT (2004), *Útügyi Műszaki Előírás ÚT 2-3.401 Közúti hidak tervezése, Általános előírások*, Magyar Útügyi Társaság, (in Hungarian).

Wolf, J.P. (1985), *Dynamic soil-structure interaction*, Prentice-Hall, Inc., New Jersey, US.

Zsarnóczay, Á., Vigh, L.G. and Kollár, L.P. (2014), "Seismic Performance of Conventional Girder Bridges in Moderate Seismic Regions", *Journal of Bridge Engineering*, **19**(5), 9 p. Paper 04014001.